Transverse cooling and heating in ion channeling

F. Grüner, W. Assmann, F. Bell, and M. Schubert
Sektion Physik, Ludwig-Maximilians-Universität München, Am Coulombwall 6, D-85748 Garching, Germany

J. U. Andersen
ACAP, Institute of Physics and Astronomy, Aarhus University, Aarhus C DK 8000, Denmark

S. Karamian
FLNR JINR, 141980 Dubna, Russian Federation

A. Bergmaier, G. Dollinger, and L. Görgens
Physik Department, Technische Universität München, James-Franck Strasse, D-85748 Garching, Germany

W. Günther
Fachbereich Physik, Universität Siegen, Siegen D-57068, Germany

M. Toulemonde
Centre Interdisciplinaire de Recherches Ions Laser, Boîte Postale 5133, 14070 Caen-Cedex 05, France
(Received 16 April 2003; revised manuscript received 7 August 2003; published 6 November 2003)

In contrast to predictions from the standard theory of ion channeling we have observed strong redistributions of initially isotropic ion beams after transmission of thin crystal foils. Depending on the experimental parameters, there can be strong enhancements, corresponding to ''transverse cooling,'' or strong reductions, ''transverse heating,'' of the ion flux along a crystal axis or plane. For most ions there is a transition from cooling to heating when the ion energy is decreased, which depends on the crystal direction and on the atomic numbers of the ion and of the crystal atoms. In this paper we present an overview of this newly discovered phenomenon. Redistribution of an initially isotropic flux violates basic symmetries in the theory of channeling. We have argued earlier that the observed transverse cooling or heating can be understood as a consequence of fluctuations in the charge state of the channeled ions, but a detailed explanation of the transition from cooling to heating has yet to be established. A theoretical description is the most difficult for ions with many electrons. A different type of simulation has been developed based on *n*-body classical trajectory Monte-Carlo procedures and the first results are discussed.

DOI: 10.1103/PhysRevB.68.174104 PACS number(s): 61.85.+p, 34.70.+e, 34.20.Cf, 34.10.+x

I. INTRODUCTION

Energetic ions entering a crystal below a critical angle relative to an axial or planar direction are guided along these directions due to correlated collisions with the crystal atoms. Under this condition of ion channeling there is a minimum distance of approach to the target atoms.[1] Thus, ions moving in a random direction probe all impact parameters, whereas channeled ions are confined to an area away from the atoms on the strings or planes.

Within the standard theory of channeling the ion motion is described with a continuum potential, but there remain fluctuations in the scattering due to thermal fluctuations in atomic positions and due to scattering by electrons. This multiple scattering fulfills a rule of reversibility or detailed balance and, as a consequence, a uniform distribution in the transverse phase space of ion motion is stable.[2,3] Since a beam which is isotropic outside the crystal populates the transverse phase space uniformly inside the crystal, and vice versa at the exit surface, an initially isotropic ion beam should not be redistributed. The violation of reversibility due to energy loss is expected to lead to intensity changes of only a few per cent, as discussed in Sec. IV.

However, our experiments show *strong* violations in the sense that, depending on experimental conditions, an initially isotropic flux can be enhanced along crystal directions by up to a factor of 4 or be reduced by a factor of 5. For the mechanisms behind these findings we have introduced the terms ''transverse cooling'' and ''transverse heating,''[4] reflecting the fact that an increase of the flux in an axial or planar direction is caused by a decrease of the ion transverse energy and, conversely, a flux reduction results from an increase of the transverse energy (heating). Since we only observe the ion exit angles, our measurements are not related to the well-known flux peaking of channeled ions, which is flux enhancement in space, not in angle. Our findings of angular flux redistributions give clear evidence of a strong violation of the rule of reversibility.

Our observations must be clearly distinguished from earlier experiments that showed flux enhancements along crystal directions due to selection effects. Most such previous studies used collimated beams in order to prepare well-defined initial conditions, and this prevents direct observation of a violation of reversibility. In some of these experiments an enhancement of the ion flux along crystal directions has been observed (so-called ''star patterns''[5]). But this

could be understood in terms of an angular spread of channeled ions, which is different from that of nonchanneled ions. Thus, dechanneled ions were spread out more than channeled ions, resulting in a flux enhancement along crystal directions. In our experiments, however, the initial condition is an isotropic flux and, according to the rule of reversibility, different strengths in multiple scattering then do not cause any redistribution. In other experiments α particles from an isotropic radioactive source have been used.[6] But, due to energy selection by the crystal or the detector, no quantitative comparison between channeled and nonchanneled particles was possible, and hence redistributions could not be measured.

When it was first discovered the effect showed a rather simple behavior. Light ions such as C or O were cooled and heavy ions such as I and Au were heated, with an intermediate behavior for Cu: cooling for well channeled ions and heating for poorly channeled ions and for ions channeled along weaker planes.[4] Fully stripped ions did not yield any redistribution, that is, in this case the rule of reversibility was not violated. However, further measurements have revealed that most ions undergo a transition from cooling to heating when the ion energy is decreased.[7] We have found that the question whether there is cooling or heating depends on several parameters, the ion energy, the crystal direction, and the atomic numbers of the ion and the crystal atoms. In this paper we present a systematic study of this phenomenon, yielding a complex overall picture. Our experiments cover a large variation in atomic numbers of ions and crystals, ions from H to Pb and crystals from Si to Pt, and a broad energy range, from a few hundred keV up to 1 GeV.

A qualitative explanation for transverse cooling and heating has been given, based on the known differences between the impact-parameter dependencies of single-electron-capture and -loss cross sections.[4] It was shown that if the mean capture radius is significantly smaller than the mean loss radius, a net loss of transverse energy follows (cooling). Heating is then associated with the opposite condition. It was later demonstrated that in case of cooling these effects can be strong enough to account for the observed flux redistributions.[8] We present measurements of charge state distributions which give a direct test of the basic assumptions of this charge-exchange model: if the mean capture radius is smaller than the mean loss radius, electron capture is more reduced for channeled ions than electron loss, and hence the charge state is expected to be shifted to higher values than for penetration in a random direction. The reversed situation should give a shift to lower charge states for channeled ions. It turns out that the charge state measurements are in accord with the charge-exchange model in case of Si and Ni crystals, but not for Pt crystals at lower velocity.

In case of multiple charge exchange per *atomic* collision, especially for heavy ions with many electrons, it can be expected that the former picture of single-electron-capture and -loss cross sections may be invalid. In order to understand and describe the ion-atom collisions better we have developed a new simulation method based on the ''*n*-body classical trajectory Monte Carlo'' (nCTMC)[9] procedure. Quantum-mechanical approaches seem impractical if not impossible due to the great mutual perturbations of the ion and the crystal atoms. Previously such nCTMC calculations have only been performed for single ion-atom collisions. Here we discuss the first results from a newly developed ''nN-CTMC'' simulation for the collision of an ion with strings of *N* atoms each carrying *n* electrons. Besides contributing to our understanding of the mechanisms of transverse cooling and heating, such simulations may lead to new insights into the old question of charge states of energetic heavy ions inside a solid.

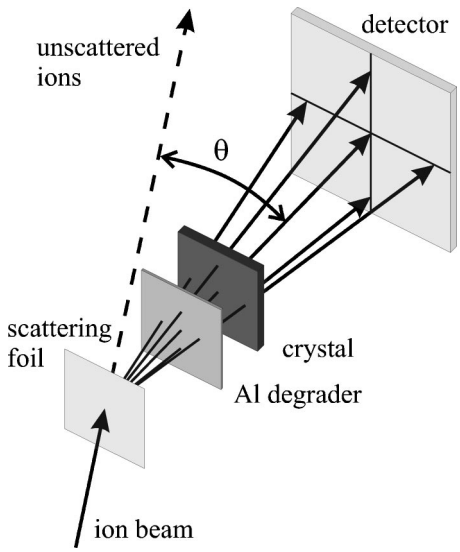

FIG. 1. Scattering geometry. The ion beam from the Tandem accelerator is scattered on thin Os or W foils, and the scattered ions are transmitted through the crystals under study. The incident ion energy is controlled by Al degraders. The ion flux behind the crystal is measured by position sensitive detectors, either an ionization chamber or a nuclear track detector, at a distance of 540 mm from the scatter foil.

II. EXPERIMENT

A. Setup

For the preparation of an initial quasi-isotropic flux the ions from the Munich 14-MV Tandem accelerator were scattered on (150–200)-μg/cm^2-thin W or Os foils. The schematic scattering geometry is shown in Fig. 1. The angle between the unscattered beam and the detector axis was as small as 12.5°, corresponding to a large Rutherford cross section for scattering and a possibility for a very large number of total counts. Self-supporting crystalline foils of 5–10 mm diameter with thicknesses in the range of a few microns were used. The Si(001) crystals with different thicknesses were produced at the Forschungszentrum Rossendorf by electrochemical etching with an ion-implanted etch stop.[10] 1.0-μm-thin Ni(001) and Pt(001) crystals were produced by molecular-beam epitaxy at the University of Aarhus. In order to avoid beam damage the crystals were mounted so far behind the scattering foil that the unscattered ions could not reach them. The ion energy before transmission was varied by insertion of thin Al degrader foils in front of the crystals.

The scattering foils, Al degraders, and crystals were mounted on a five-axis positioning system in a high-vacuum chamber. The ion flux after transmission through the crystals was detected by a position sensitive ionization chamber.[11] For ion energies below the threshold of the chamber a CR39 plastic detector was used.[12] Ion tracks in the CR39 foils were made visible by etching in a NaOH bath, after which they were scanned in an automatic microscope with a pattern recognition system at the University of Siegen.[13] In this case the raw data consist of a list of detected tracks, from which it is possible to infer the ion flux distribution.

The advantage of the ionization chamber is the possibility of getting results on-line, but its disadvantages are a relatively high-energy threshold and electronic artifacts due to inhomogeneities of the electrical field inside the detector that must be corrected for. Reproduction measurements with CR39 and the ionization chamber showed that these artifacts can be accounted for and have no influence on our results. For both detector systems the angular resolution was found to be better than the angular width of the observed phenomenon which has half angles down to about 0.05°. The detector solid angle was 7 msr for both systems. All given exit energies in this paper are mean energies, either measured directly by the ionization chamber or calculated in the case of measurements with CR39.

B. Angular distributions

The signals from the ionization chamber allow the calculation of a two-dimensional position spectrum, which resembles the angular emission pattern of the transmitted ions. Due to distortions of the electrical field inside the chamber one must apply several corrections to these raw data in off-line analysis. For a scattering angle of only 12.5° there is a variation of a factor of 3 in the scattering cross section within the solid angle of the detectors. An off-line routine was developed to yield flux distributions corresponding to an isotropically scattered beam. It turns out that the correction follows the angular dependence of Rutherford scattering for Si and Ni crystals but for Pt crystals the Rutherford distribution is smeared by the greater multiple scattering. The validity of the Rutherford correction by an angular dependent factor was verified by an experiment under a scattering angle of 50°, where the variation of the Rutherford cross section is negligible. The resulting angular distribution was the same as in another experiment with the same exit energy under the usual scattering of 12.5° after the Rutherford correction.

The final axial and planar angular distributions were then generated by circular averaging of the position spectra around an axis or by averaging along a plane (where other planes in the position spectra were left out by a cut). The resulting dependence of the counts $\chi(\psi)$ on the transmission angle ψ relative to an axis or plane was normalized to the counts at large angles, far from axes and planes. $\chi(0)$ then gives the factor by which the number of well channeled ions is increased or reduced compared with the initial value.

C. Charge state distributions

In order to study charge state distributions of channeled vs nonchanneled ions in the cooling and heating energy regimes we used beams of 240-MeV and 100-MeV Ag ions, respectively. The experiments were made in transmission geometry. For a definite comparison of mean charge states of channeled vs nonchanneled ions we prepared a well collimated beam with a divergence of about 0.01°, a beam-spot size of about 100×100 μm^2, and a beam intensity of only a few thousand particles per second in order to prevent beam damage to the crystal.[14] A crystal axis was aligned with the beam direction by observation of the energy loss which is less for channeled ions than for nonchanneled ions. The charge state distributions of the ions exiting the crystals were measured with a Q3D magnet spectrograph.[15] The acceptance angle was large enough that all ions entering the crystals were detected. From other measurements[16] it is known that charge state equilibrium is reached within the thickness of our crystal foils both for channeled and random ions, independent of the initial distribution.

III. RESULTS

We have made measurements for a variety of ions over a large range of ion energy. The use of different crystals allows a study of the dependence of the effect on the atomic number of the crystal atoms, and the dependence on the channel dimensions and the strength of the channeling potential can be studied by a variation of the orientation of the crystal. Measurements for different crystal thicknesses show how the effect increases with increasing path length. The variation with the ion charge state cannot be tested independently, because the entrance charge state distribution is determined by the charge state distribution after the scattering foils, and within the crystals an energy dependent mean equilibrium charge state is reached after about 1000 Å,[16] which is rather short compared to the total thickness of our crystals.

We first report on measurements of flux distributions displaying transverse cooling and/or heating for each of the three crystals and then on measurements of charge state distributions.

A. Cooling and heating

1. Si crystals

a. Energy variation. A study of the dependence of cooling/heating on ion energy requires on one hand a sufficiently small crystal thickness to give an acceptable energy resolution, and on the other hand a sufficiently large thickness to give a significant angular flux redistribution. The optimum thicknesses is about 3 μm for Si(001) crystals. The ion energies used ranged from a few hundred keV for protons up to 1 GeV for Pb ions. Typical energies available from the Tandem accelerator are (0.5–3.0) MeV/u. 1-GeV Pb ions were provided at the GANIL accelerator in Caen, France, and the proton beam at the MPI/IPP (Max-Planck Institute for Plasma Physics, Garching, Germany). In the latter measurements the flux distributions were recorded with nuclear track detectors.

Figure 2 shows angular flux distributions of Y ions around the Si $\langle 100\rangle$ axis at three different exit energies, measured with the ionization chamber, and the corresponding axial an-

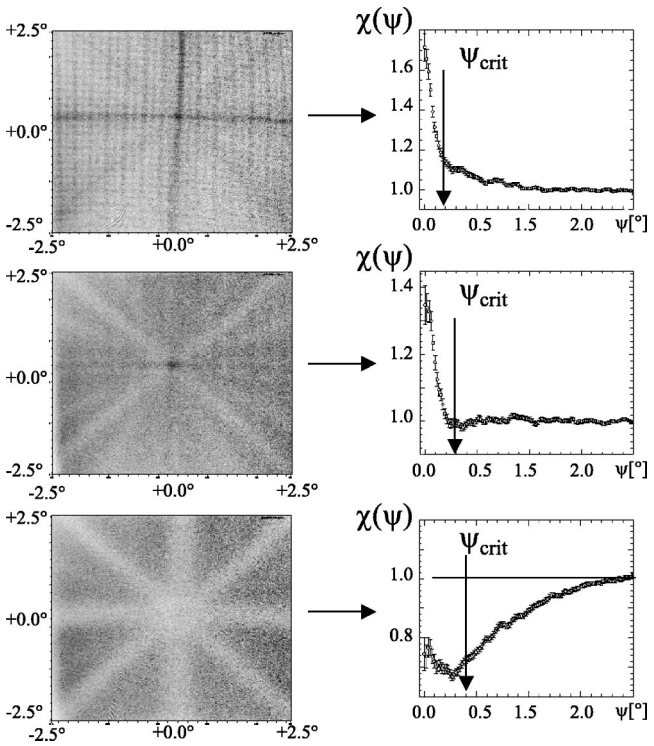

FIG. 2. Angular flux distributions of Y ions after transmission of a 3.4-μm-thin Si(001) crystal, and corresponding circular averages around the $\langle 100 \rangle$ axis at varying polar angle. The exit energies are from top to bottom, 177, 117, and 63 MeV. The top part shows a clear cooling case, the bottom a clear heating case, and the middle part an intermediate stage. The HWHM of the first two angular distributions are $(0.09 \pm 0.01)°$ and $(0.10 \pm 0.01)°$, and the corresponding critical Lindhard angles are 0.23° and 0.28°.

gular distributions. The top part of the figure displays a case with strong flux enhancements along all visible crystallographic directions, i.e., a cooling case. In contrast, the bottom part shows a heating case with strong flux reduction along the crystal directions. The axial flux redistributions extend far beyond the critical Lindhard angle for channeling,

$$\psi_1 = \sqrt{\frac{2Z_1 Z_2 e^2}{4\pi\epsilon_0 E d}}, \tag{1}$$

where E is the ion energy, Z_1 and Z_2 the atomic numbers of the ion and the crystal atoms, and d the interatomic spacing along the axial direction. For the example shown in Fig. 2, ψ_1 is 0.23° in the cooling case and 0.28° for the heating case. In case of cooling the half angle (half-width at half maximum, HWHM) of the measured angular distribution is 1/2.6 of the critical angle, and experiments with other ions show that this ratio is in general between 1/3 and 1/2. The middle part of Fig. 2 displays the transition stage from cooling to heating. This stage is characterized by an axial flux enhancement that is only visible at angles smaller than the critical angle. In order to consistently characterize cooling and heating we introduce a volume measure V:

$$V = 2\pi \int_0^{\psi_{max}} [\chi(\psi) - 1] \psi d\psi, \quad \psi_{max} \gg \psi_1 . \tag{2}$$

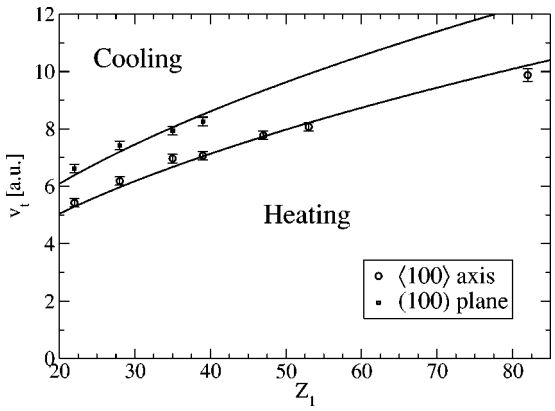

FIG. 3. Transition velocities v_t in atomic units for all measured ions in case of Si-crystal along $\langle 100 \rangle$ axis and along (100) planes. Both lines are fits according to $v_t = \alpha Z_1^{1/2}$, with $\alpha_{axis} = 1.13 \pm 0.01$ and $\alpha_{plane} = 1.36 \pm 0.02$.

This gives an overall measure of the angular flux redistribution. We define cooling by $V > 0$ and heating by $V < 0$. The exit energy for a case where the volume measure V equals zero defines the so-called "transition energy" E_t, and from that we get the corresponding "transition velocity" v_t. Thus, the transition energy for Fig. 2 is slightly below the exit energy of the middle case. A compilation of all axial transition velocities is presented in Fig. 3. A fit of these data reveals that $v_t \approx 1.13 v_0 Z_1^{1/2}$ (with v_0 being the Bohr velocity), and, correspondingly, the transition energies scale with Z_1^2 ($E_t = \frac{1}{2} m v_t^2 \sim Z_1 v_t^2$). Note that a fit according to a scaling of v_t with $Z_1^{2/3}$ yields a χ^2 deviation from the data, which is larger by one order of magnitude than the $Z_1^{1/2}$ scaling. Furthermore, if one looks up tabulated charge states[17] behind solids at the measured transition energies, one finds that the mean charge state Q_t at the transition is about 60% of the nuclear charge for all observed ions. A remarkable feature is the relatively narrow velocity region in which the transition occurs. Within a velocity range of $\Delta v / v \approx 15\%$ the transition from a coolinglike angular distribution to a heatinglike one is clearly seen (see Fig. 7). We have seen that the width of the exit energy distributions of about 10–15 % due to energy straggling in the Al degraders and Si crystals have no remarkable effect on the energy dependence of the angular distributions.

With the above definition the distinction between overall cooling and heating depends mainly on the behavior of ions with angles above the critical angle. In this region the transverse motion samples all impact parameters with the string atoms, but the ions are still channeled in the sense that their motion is to a large extent governed by the continuum channeling potential, and electron capture and loss can therefore modify the angular distribution.

Experiments with O and C ions showed that the angular flux redistributions completely disappear if the mean charge is close to the nuclear charge, e.g., for O ions with mean charge larger than $\langle Q \rangle = 7.9$. The case for S ions is displayed in Fig. 4. The mean charge state near the high-energy end is about 15^+.[17] On an average, the S ions only carry one electron, and the cooling strength $\chi(0)$ is very much reduced.

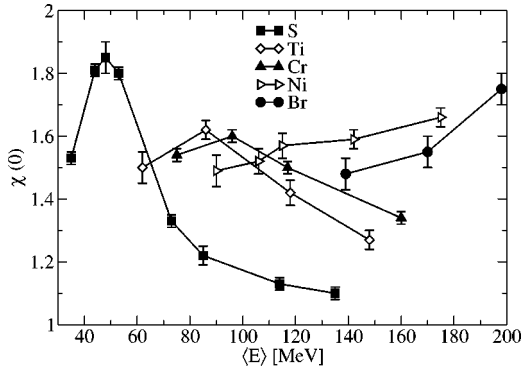

FIG. 4. Axial cooling strength $\chi(0)$ plotted against mean energy $\langle E\rangle = 0.5(E_{in}+E_{out})$ for $E \gg E_t$ of several ions behind 3-μm Si crystals (lines are drawn to guide the eye).

These findings are in accordance with the predictions of the charge-exchange model. The energy available with the Tandem accelerator is not high enough to produce fully stripped ions heavier than S. The plots in Fig. 4 of the cooling strength $\chi(0)$ against ion energy exhibit a clear maximum for S, Ti, and Cr while there is a slight increase with increasing energy for Ni and Br but no indication of a maximum. However, if the energy at the maximum scales approximately with the square of the ion atomic number, such as the transition energy, the maxima should be close to or above the highest beam energies used.

A very intriguing experimental finding is the absence of the transition from cooling to heating for all ions lighter than Ti: *p*,[18] He,[19] C, O, F, S, and Ca ions show no heating even at exit energies significantly below the extrapolation of the measured transition energies to lower atomic numbers $Z_1 < 22$. The measurements were for 120-keV *p*, 0.5-MeV He, 7-MeV S and F, and 22-MeV Ca. The flux distribution of the 7-MeV S case is shown in Fig. 5. Strong flux enhancement is

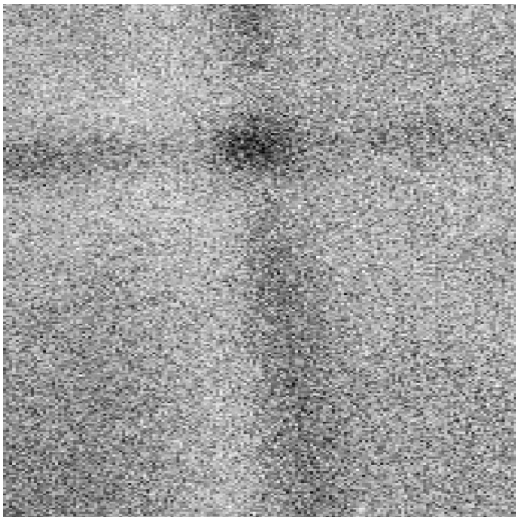

FIG. 5. Flux distribution of S ions behind a Si crystal with an exit energy of 7 MeV. The ⟨100⟩ and the (110) plane show strong flux enhancements embedded in a region with flux reduction, but still the volume measure is positive, indicating an overall cooling effect. No flux redistributions are seen for the (100) planes.

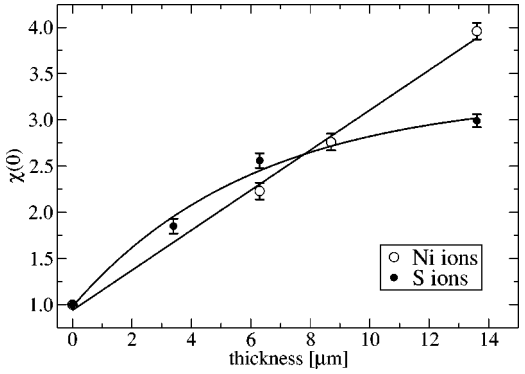

FIG. 6. Thickness dependence of the cooling strength in the case of S ions (filled circles, at the same exit energy of 57 MeV) and Ni ions (open circles, with the same entrance energy of 187 MeV). Whereas the first show a saturation behavior, the latter show a linear increase.

seen for the ⟨100⟩ axis and the (110) plane, in both cases embedded in a zone of flux reduction but with a positive volume measure. The weaker (100) plane shows heating, whereas in other cases this plane can also completely disappear.

b. Thickness variation. We have studied the cooling strength $\chi(0)$ as a function of the crystal thickness for O, S, Ti, and Ni ions. This requires two conditions to be fulfilled: First, the entrance ion energy must be large enough so that after transmission the exit energy is significantly above the corresponding transition energies and, second, the entrance energy must not lead to fully stripped ions, otherwise the cooling effect would also be decreased and thus the thickness dependence would be distorted.

Measurements for S and Ni ions are shown in Fig. 6. Because the ion energy decreases nearly linearly with depth in the crystal, the thickness dependence is linked to the energy dependence, and this complicates the interpretation. However, for Ni the enhancement was found to be nearly independent of energy (Fig. 4) and the observed linear increase of $\chi(0)$ with thickness has a simple interpretation: there is a steady accumulation of flux at small angles and the multiple scattering which smears the angular flux distribution is too weak to be significant. For the lighter S ion the enhancement is seen to saturate, and this may be due to a combination of the influence of multiple scattering and the reduction of the enhancement at high energies seen in Fig. 4.

c. Variation of crystallographic directions. The flux distributions of Y ions around the ⟨100⟩ axis are compared with the (110) planar distributions in Fig. 7. The Lindhard critical angle is, for a given energy, smaller by about a factor of 3 for the planar case. At lower energies there is a stable ''shoulder'' in the planar cases which is probably due to an accumulation of heated ions that are not transferred quickly enough to higher angles, and these shoulders make it more difficult to distinguish between cooling and heating in the planar case. In contrast, cooling and heating are easily distinguished in the axial case from the slope of the angular flux distributions above the critical angle.

The transition behavior of the weaker (100) planes is fairly simple as the transition stage shows a clear disappear-

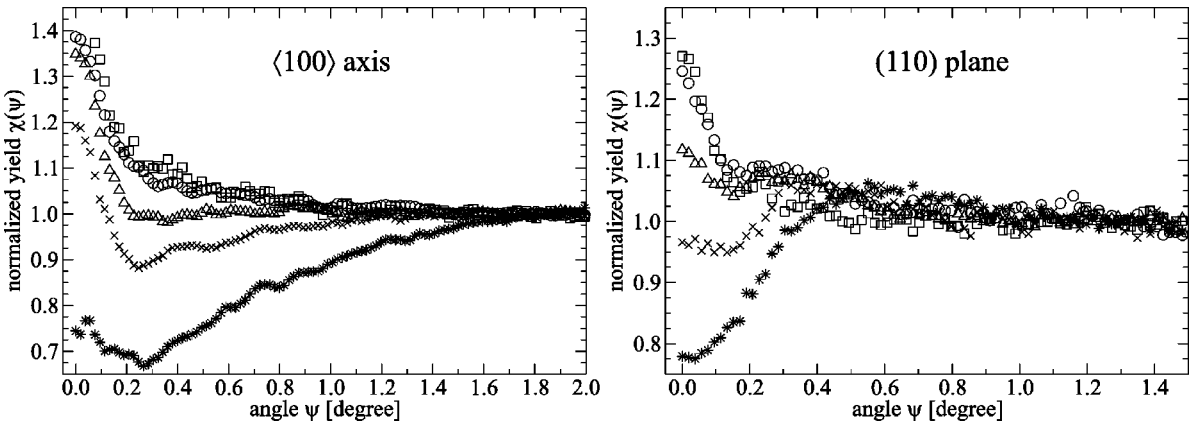

FIG. 7. Axial and planar angular distributions of Y ions after transmission of a 3.4-μm Si(001) crystal. The exit energies are 177 (squares), 141 (circles), 117 (triangles), 92 (crosses), and 63 MeV (stars).

ance of any flux redistribution across the planes. The transition energies are significantly higher than in the ⟨100⟩ case, as indicated in Fig. 3.

The ⟨110⟩ axis was probed with Ni, Br, Y, and Ag ions. In general, the cooling strength is larger by about 30% as compared with the ⟨100⟩ axis. However, no transition to flux reduction of channeled ions was found. Even 5-MeV Ni ions still show a cooling pattern but with the addition of a ''depletion zone'' around the axis as displayed in Fig. 8. There are two important differences between the ⟨100⟩ and ⟨110⟩ axes: the spacing of atoms along the strings is smaller by a factor $1/\sqrt{2}$ for the ⟨110⟩ axis and this means that the critical angle is larger. In addition, the ⟨110⟩ strings are arranged in closelying pairs which in effect doubles the area of the channels in between. Orientation of the crystal for transmission along the ⟨110⟩ axis allows a study of the strong (111) planes that also show no transition behavior.

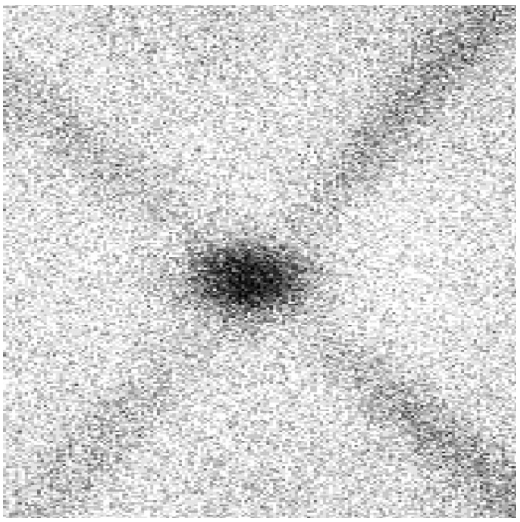

FIG. 8. Flux distribution of Ni ions with 5 MeV exit energy after transmission of a 2.9-μm-thin Si crystal oriented along the ⟨110⟩ axis. Clearly cooling is seen, both for the axis and for the (111) planes, but no heating as for the ⟨100⟩ axis at this energy.

2. Ni crystal

The transition velocities (in atomic units) for the ⟨100⟩ axis are 7.50 ± 0.15 for Br, 7.98 ± 0.14 for Y, and 8.65 ± 0.18 for I ions. Thus, they are significantly higher than the corresponding values for Si⟨100⟩. Figure 9 shows axial angular distributions of Ni, Cu, and Zn ions, all with the same exit energy of about 40 MeV. A significant change is seen in the behavior between the best channeled ions of Ni and Cu on one hand and of Zn and Ge (not shown, but similar to Zn) on the other. Whereas the former ions remain in an intermediate stage, the latter undergo a clear transition to strong flux reduction as for Si⟨100⟩ crystals (compare Fig. 7). The behavior of Ni ions at much lower energy was observed to be qualitatively similar to that at 40 MeV, i.e., the flux of the best channeled ions is never as strongly reduced as for Zn ions. It is again remarkable that neighbors in the periodic table are found to behave quite differently.

3. Pt crystal

Qualitatively different results for the flux redistribution are found for transmission through a Pt crystal, as illustrated

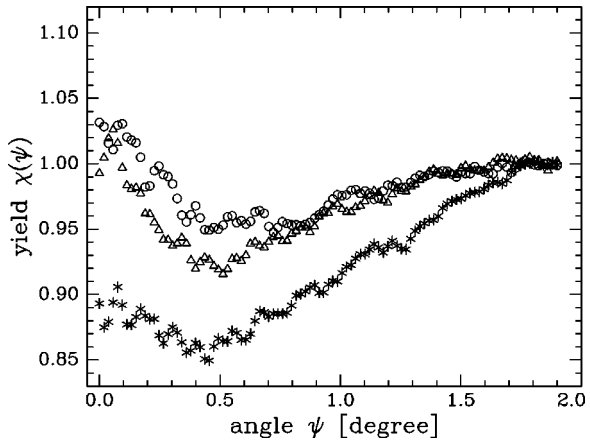

FIG. 9. Axial angular distributions of Ni (circles), Cu (triangles), and Zn (stars) ions after transmission of a 1.0-μm Ni(001) crystal at the same exit energy around 40 MeV.

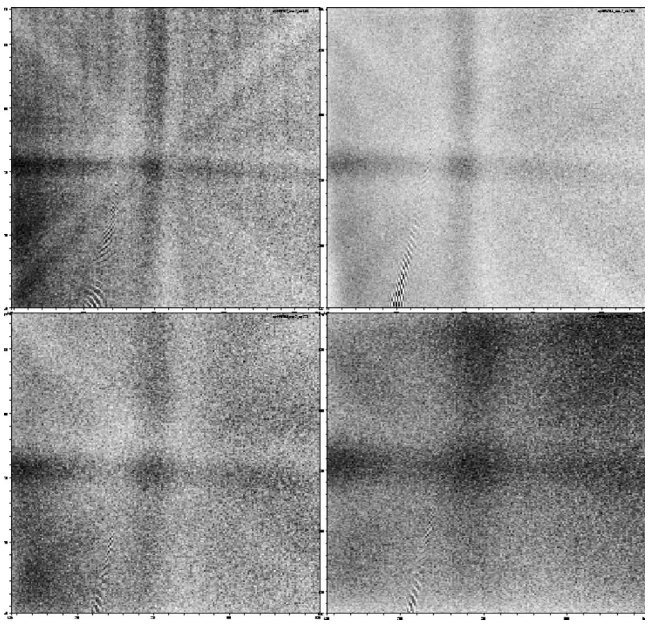

FIG. 10. Flux distributions of Br ions transmitted through a 1.0-μm Pt(001) crystal at four different exit energies: 96 MeV (top left), 58 MeV (top right), 42 MeV (bottom left), and 27 MeV (bottom right). There is strong flux enhancement embedded in a depletion zone at all energies. The widths of the regions with flux enhancement scale with the critical angles, which are 0.83°, 1.06°, 1.25°, and 1.56°, respectively. The shown angular windows are about 4° in both directions.

in Fig. 10 by angular distributions of Br ions transmitted through a 1-μm-thick Pt$\langle 100 \rangle$ crystal at four different energies. At all energies a strong flux enhancement is embedded in a depletion zone, and the volume measure V defined in Eq. (2) is close to zero. So the main effect appears to be strong cooling for well channeled ions. Figure 11 shows a comparison of the angular distributions of Ag ions with about the same exit energy behind a Pt and a Ni crystal. It is seen that at about the same velocity, and thus for about the same mean random charge state,[20] the behavior depends strongly on the crystal material.

Experiments with 1-GeV Pb ions at GANIL showed that there is no transition to clear heating even in the case of very heavy ions with an exit energy (320 MeV) well below the corresponding transition energy for a Si$\langle 100 \rangle$ crystal of 500 MeV. Even heavy ions such as (122 MeV) Th ions did not show clear heating but a cooling pattern embedded in a depletion zone.

Thus, we conclude that the observed flux redistributions are qualitatively different for Pt crystals as compared to Si and Ni crystals. A strong flux enhancement of well channeled ions embedded in a depletion zone is observed in general for Ni, Br, Y, Ag, I, Au, Pb, and even Th ions. Measurements with Ag and Au ions channeled along the $\langle 110 \rangle$ axis also do not show a transition to heating at low energies.

B. Charge state distributions

The mean charge states of Ag ions channeled along $\langle 100 \rangle$ axial and (110) planar directions in a Si crystal, and along a (100) planar direction in Ni and Pt crystals, are compared with the mean charge state for transmission in a random direction in Table I. For all crystals the mean charge state for channeled ions is higher at high energy (cooling regime), and the relation is reversed at low energy (heating regime).[14] For Si and Ni crystals these findings are in accordance with the charge-exchange model. However, the Pt case is different since there is overall neither cooling at high energies nor heating at low energies according to our definition in terms of the volume measure in Eq. (2) (see also Fig. 11). Instead, there is strong cooling of well channeled ions at all energies. Hence, the charge-exchange model implies a shift to higher charge states at small exit angles. We thus performed more detailed charge state measurements by tilting the Pt crystal from the best alignment to a random direction. However, we could not select exit angles, but the tilting was performed with a large acceptance window detecting all exit angles, whereby a strong positive charge state shift at small angles

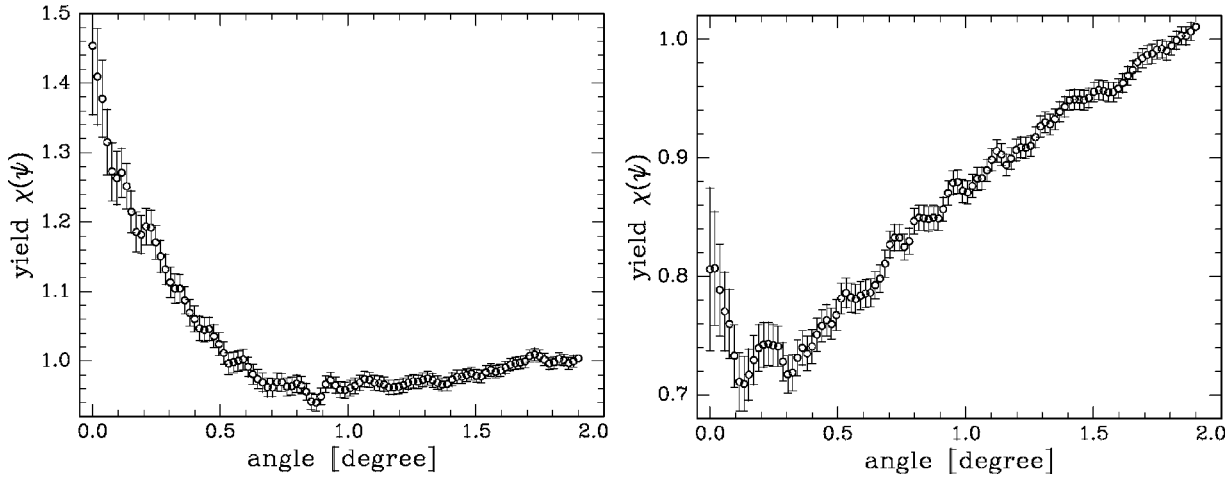

FIG. 11. Axial angular distributions of Ag ions with the same exit energy around 66 MeV after transmission of a 1.0-μm Pt(001) crystal (left) and of a 1.0-μm Ni(001) crystal (right). Whereas the Pt case shows strong flux enhancement embedded in a depletion zone, clear heating is seen for the Ni case. The critical angles are 1.18° and 0.71°, respectively.

TABLE I. Mean random charge states Q_{random} and shifts ΔQ_{axis} and ΔQ_{planar} of mean channeling charge states in respect to the random value. The mean channeling charge state is lower (higher) than the mean random charge state, if the velocity v is low (high).

Ion	v (a.u.)	Crystal	Q_{random}	ΔQ_{axis}	ΔQ_{plane}	Regime
100-MeV Ag	6.15	Si	21.04 ± 0.03	-2.25 ± 0.06	-2.35 ± 0.06	heating
240-MeV Ag	9.52	Si	24.09 ± 0.03	$+2.02 \pm 0.06$	$+0.90 \pm 0.06$	cooling
100-MeV Ag	6.15	Pt	20.40 ± 0.05	-0.79 ± 0.06	-0.34 ± 0.06	cooling
220-MeV Ag	9.12	Pt	25.98 ± 0.03	$+0.80 \pm 0.06$	$+0.26 \pm 0.06$	cooling
100-MeV Ag	6.15	Ni	21.20 ± 0.05	-0.73 ± 0.06	-0.45 ± 0.06	heating

could be smeared out. Figure 12 displays the mean outgoing charge states $\langle Q_{out} \rangle$ plotted against the tilt angle for axial channeling of low-energy Ag ions through the Pt crystal. Averages over two different groups of ions are plotted: over all detected ions, and only over the ions with the lowest-energy loss, that is, over the best channeled ions. A third possibility, which is not shown as the results are very close to the first case, is to include only the ions with energy near the maximum in the exit energy distribution for each tilting angle. The idea is that such a cut selects ions with an average transverse energy close to that given by the incidence angle and hence excludes distortions due to dechanneling. Even though there is an indication, with the first and third type of analysis, of a small decrease of the charge state vs angle near zero tilt, it is not clear that the results are consistent with the observed strong cooling of well channeled ions in Pt crystals.

IV. THEORETICAL APPROACHES

In view of the complexity of the reported effects no simple explanation can be expected. The most challenging finding is the relatively sharp transition from cooling to heating with decreasing ion energy, and its dependence on the combination of atomic numbers of the ion and the crystal atoms and on the crystallographic direction. Below, we first discuss the relation of the observed angular flux redistributions to the rule of reversibility in channeling. We then consider the charge-exchange model in which the effects are explained as a consequence of the irreversible processes of electron capture and loss. Some of the general features of the observations are in accord with expectations based on this model, but there are also inconsistencies. It is one of the most interesting aspects of the measurements that they may provide new insight into the old problem of the charge states of energetic heavy ions inside a solid. The situation is complex for ions which carry many electrons and may be highly excited. To obtain some insight in this region into both the charge exchange and its influence on the deflections of the ion in collisions with crystal atoms we have introduced a different approach with intensive nCTMC-type computer simulations that calculate the complete dynamics of all interacting particles within classical physics.

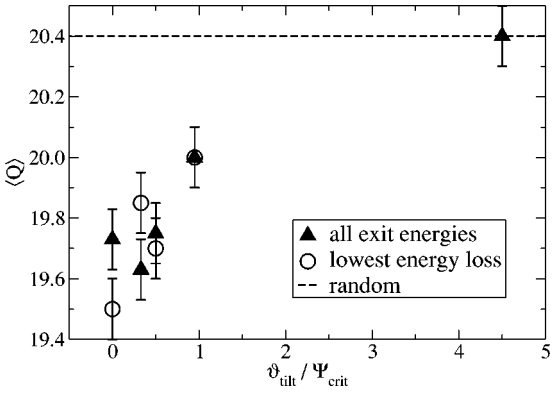

FIG. 12. Tilting of Pt(001) crystal with 100-MeV Ag ions: Mean ⟨100⟩-axial channel charge states plotted against the tilting angle in units of the critical angle for axial channeling, once averaged over all ions (i.e., all exit energies), and once only for channeled ions (lowest-energy loss). In the first case a negative slope, which, according to the charge-exchange model, would indicate cooling, around zero tilting is seen. The horizontal line corresponds to the random value.

A. Violations of reversibility

Ions moving through a crystal at a small angle to a major axis are guided by an effective transverse potential corresponding to an average of the ion-crystal static potential over the coordinate parallel to the axis, and thus there is approximate conservation of the transverse energy equal to the sum of this potential and the kinetic energy in the transverse motion. For angles smaller than the critical angle in Eq. (1) the ions are confined to move in the channels between the atomic strings, and they are said to be channeled. Due to multiple scattering on electrons or thermally vibrating atoms there are transitions from channeled to nonchanneled motion and vice versa, which may be described as a diffusion in transverse energy.[3] A general rule of reversibility in channeling states that this diffusion is symmetric, in the sense that the probability for diffusing from a small transverse energy to a large one is identical to the probability for the reverse process (with a correction for the change in the accessible area in the transverse plane). For multiple scattering on electrons the basic symmetry leading to this reversibility is a symmetry of the scattering in momentum space.[2] In the case of multiple scattering due to thermal displacements of atomic nuclei reversibility may be derived from time reversal, which evidently is violated by inelastic-scattering processes or any process which contradicts conservative forces.

The observed redistributions in angle of the ion flux after transmission through a crystal are evidence for a strong violation of the rule of reversibility. A well-known source of

irreversibility is the energy loss of the ions. The multiple scattering is Coulomb scattering with a cross section that increases with decreasing energy. Because channeled ions suffer less energy loss than nonchanneled ones, their angular spread by multiple scattering is smaller, and the difference can be estimated from the energy dependence of Rutherford scattering. The conclusion is that the relative flux redistributions cannot be much larger than the relative energy difference between channeled and nonchanneled ions, which is in our cases of the order of 10%.[14] In addition, the violation of the reversibility by energy loss can only lead to an enhancement of the flux of channeled ions, and thus it cannot explain heating at all. Finally, we have observed that there is no flux redistribution for fully stripped ions, and this means that the rule of reversibility is obeyed in this case, irrespective of the presence of energy loss.

A qualitative explanation of the observations has instead been proposed in a time asymmetry of fluctuations in the ion charge state. The deflection angle in ion collisions with crystal atoms depends on the ion charge state and this may be taken into account by the introduction of a charge state dependent channeling potential. Owing to the fluctuations in charge, the potential then becomes time dependent in the sense that it depends on the position of charge change, which means that if the ion charge state is different when it approaches and leaves a crystal string or plane, the motion becomes irreversible. Such a difference results when the probabilities for electron capture and loss in a collision with a crystal atom have a different dependence on the impact parameter.

B. Charge-exchange model

For an energetic heavy ion penetrating a solid there is a dynamic equilibrium between capture and loss of electrons and the charge state fluctuates around an equilibrium value. The impact-parameter dependencies for capture and loss are different because the processes are not related by time reversal: electrons are captured from bound states but lost to the continuum. This leads to a difference between the charge state distributions for channeled and random ions, as reported elsewhere[16,21] and also in the present paper. If the mean exit charge state of channeled ions is higher than in a random direction, it can be concluded that the probability of electron capture decreases faster with increasing impact parameter than electron loss, and that therefore the mean capture radius is smaller than the mean loss radius.

The suggested mechanism for focusing of the flux in the direction of an axis (or plane) may be explained as follows:[4,8] If an electron is captured at a distance r_c from a string and lost at a larger distance r_l, the electron is carried away from the row of crystal atoms, up a potential hill, and the ion transverse energy is decreased by $\Delta E_\perp = U_p(r_l) - U_p(r_c) < 0$, assuming that the string potential $U(r)$ is proportional to the ion charge Z_1^*, i.e., $U(r) = Z_1^* U_p(r)$, where $U_p(r)$ is the string potential for a proton. Therefore, if the capture distance is on an average smaller than the loss distance, transverse cooling occurs, and the reverse of this condition leads to transverse heating.

Within the energy range of our experiments the dominant capture process even at larger impact parameters is mechanical electron capture, while radiative electron capture (REC) is negligible. This can be seen from a comparison of measured REC cross sections[22] and capture probabilities at relatively large impact parameters compared with nCTMC simulations.[9] It may be shown from simple considerations of the energy-momentum balance, and has been confirmed by experiments[23] that mainly inner-shell electrons are captured at very high ion velocity and that this capture can only take place in a collision with a target atom at a very small impact parameter. There is not a similar confinement to small impact parameters of projectile ionization in this limit, and hence it is expected that the average capture radius becomes smaller than the average ionization radius. This is in agreement with the general observation of cooling at high ion energies.

Also, the observed energy dependence of the cooling strength is qualitatively in accord with this picture (see Fig. 4). The maximum should be at a velocity where a substantial fraction but not all of the ion electrons are stripped off; e.g., according to the Shima tables[17] the equilibrium charge state for 50-MeV S ions ($Z_1 = 16$) is about 11.2. The equilibrium charge state roughly corresponds to removal of all electrons with binding velocities lower than the projectile velocity. Since the binding velocities scale with $Z^{2/3}$ in the Thomas-Fermi description of atoms, this argument leads to an expected approximate scaling of the ion energy at the maximum with $MZ^{4/3}$, and this is close to the scaling of the transition energies found.

At ion velocities which are not much higher than typical binding velocities the physics of electron capture onto a highly charged ion is not determined by the energy-momentum balance but may instead be described by concepts introduced by Bohr and Lindhard,[24] which were also used in the first discussion of the charge-exchange model and found to be consistent with the observations at that time.[4] Whereas this charge-exchange picture is likely to be valid at high ion velocity where only few bound electrons are left, it fails at low velocities and has, in particular, problems in explaining the sharp transition between the cooling and heating regime: From an atomic physics point of view it is hard to understand that within a 15% change of the ion velocity a drastic change of the impact-parameter dependence of capture and loss mechanisms should occur. The complexity of this phenomenon is seen also from the observation that in many cases the transition does not occur, such as for ions with low atomic number and, in general, for the very open $\langle 110 \rangle$ direction in Si.

The measurements with a Pt crystal gave qualitatively different results from those obtained for Si and Ni. The volume measure defined in Eq. (2) was found to be close to zero for all energies, but there was an enhancement of the flux at small angles, corresponding to cooling for well channeled ions. To some extent the lack of cooling or heating at angles near the critical angle for channeling may reflect the much greater multiple scattering for this high-Z crystal. As mentioned in Sec. II, the multiple scattering is strong enough to give some deviation from the Rutherford scattering law. In addition, the dependence on ion charge state of the deflection

angle in a close ion-atom collision may be considerably weaker in Pt than in the lower-Z crystals because of the presence of the large number of target electrons. In collisions with large impact parameter on the other hand, the charge state could still be important. On the other hand, it may also be the case that for Pt target the direct proportionality of the ion-crystal potential on the ion charge could be invalid. Furthermore, the observation of cooling for well channeled ions also at low ion energies appears to be in conflict with the charge state measurement (see Fig. 12).

Summing up, we have presented evidence for cooling of light ions by charge exchange at high projectile velocities. The phenomena observed for ions with many electrons are much more complex and only tentative explanations have been given. But this is perhaps the most interesting situation because we may learn something new about charge states in solids from a further theoretical analysis. This is the motivation for the simulations described in the following section.

C. nN-CTMC simulations

Swift heavy ions cause a great perturbation of the target electron system by immense ionization and polarization processes. Due to the impracticality of a quantum-mechanical treatment of this many-body problem an nCTMC-type[25] approach is developed. This procedure has been successful in reproducing measurements of single-ion-atom collisions in gases at comparable energies,[9] and hence it looks promising to extend this procedure to collisions of ions inside a crystal.

Within the CTMC model the system under study is treated as a classical system with initial conditions derived from quantum mechanics.[26] In this sense it is an *ab initio* calculation where there is no free parameter that can be fitted to experimental data. The n-body CTMC procedure takes into account all interacting particles, thus describing the complete dynamics of the system. Only the interaction between bound target electrons is not explicitly calculated, however, the presence of other bound electrons is implicitly entailed via screened nuclear charges in the electron-atomic nuclei interactions.[9] Target electrons are distributed around the atomic nucleus according to a microcanonical distribution and initially quantized energy levels, but quantization is not preserved thereafter.

As an extension of existing nCTMC simulations of single-ion-atom collisions we have developed a nN-CTMC simulation for the interaction of an ion with two parallel strings of N crystal atoms each carrying n electrons.[27] Additional concepts were introduced to account for multiple collisions of the ion with the target atoms, for instance, interactions between bound *ionic* electrons as well as between ionic and atomic bound electrons. Such time consuming calculations are made possible by the increased computer power available. In all simulations performed so far the ion interacts simultaneously with two strings each carrying four Si atoms separated along the string by 5.43 Å, with a distance of 1.92 Å between the two strings. The initial condition for the ion is a bare ion with an effective nuclear charge set to a value significantly above the equilibrium charge state expected inside the ''solid.'' When moving along the strings the ion

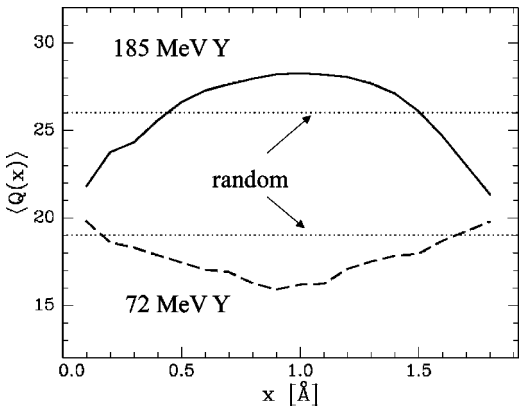

FIG. 13. Simulated mean charge states of Y ions as a function of the transverse position between the two atomic strings at two different energies: 185 MeV (solid line) and 72 MeV (dashed line). In correspondence to our measurements the charge state of the best channeled ions is higher (lower) at high (low) energy than the average over all impact parameters, see also Table I. The corresponding tabulated random charge states for the two energies behind a thin C foil (horizontal lines) are 26.0 and 19.0, respectively (Ref. 17). The random values for Si can be expected to be lower by about one unit (Ref. 20).

experiences electron capture and loss, thus building up an entourage of bound electrons, i.e., electrons with negative total energy in the ion frame. In order to keep the computation time as low as possible the ion is confined to move in the plane between the two strings, whereas all electrons can move in three dimensions. Each time an ion passes the third atom in a string, the two atoms at the back end of the two strings are removed, while two new atoms are placed in front.

As a first basic check of the validity of the simulations we have compared test results with tabulated charge state distributions behind thin carbon foils and energy-loss values for amorphous materials and have found very good agreement. These findings will be reported in a separate study of charge states inside solids and the corresponding stopping powers.[27]

First results of these calculations reproduce qualitatively the observed shifts in the charge state at high and low velocities. In Fig. 13 mean charge states, defined from the average number of bound electrons on the ion, are plotted against the transverse position in the channel. At high velocity the mean channeling charge state is higher than a supposedly random charge state (averaged over all impact parameters), and there is a shift to lower channeling charge states at low velocity. Moreover, the mean charge states averaged over all impact parameters are fairly close to measured mean random charge states in thin carbon foils,[17] which should be comparable for Si foils.[20] Furthermore, we found that from each atom several electrons are captured into highly excited states, as compared to known values of binding energies in the ion ground states. They are easily removed in the collision with the next atom, thus leading to a situation of multiple charge exchange in one atomic collision. For low velocity the number of charge exchanges is so large that a local charge state equilibrium is nearly reached at each impact parameter.

The observed shifts of channeling to random charge states can be explained with the help of the simulations in the following way. At high velocity the major characteristic is the capture of the relatively strongly bound Si *L* electrons at small distances, as discussed in the preceding section. In the middle of the channel there is no capture but still loss due to electron-impact ionization by the loosely bound Si *M* electrons. Hence, the mean charge state of channeled ions should be greater than the one for random ions which probe all impact parameters. This is in accordance with the charge-exchange model and confirmed by the measurements of charge state distributions at high velocity. At low velocity, however, a different characteristic appears: effective capture from larger distances is observed, and as these captured electrons are less strongly bound, the major factor for determination of the charge state is now the electron-electron scattering. In the middle of the channel electron-impact ionization is less effective, so that lowest charge states can only survive in this region. Thus, for low velocities the channeling charge states should be lower than along random direction, in agreement with the measurements.

These calculations also allow a determination of the ion scattering angles in collisions with atoms and hence a determination of cooling or heating of the ion beam. However, this requires much larger statistical ensembles than used in these preliminary calculations of charge state distributions. It looks promising to continue these very time consuming calculations to try explaining some of the puzzling features of the observed cooling and heating phenomena, and thereby also to get a better understanding of charge states of heavy ions in solids.

V. SUMMARY

We have presented a systematic study of the transverse cooling and heating effect in ion channeling, varying the ion energy, the crystal direction, and the thickness and atomic number of the crystal. Depending on these variables either strong enhancement (cooling) or reduction (heating) of the ion flux along crystallographic directions were observed. Ions with higher atomic number than the crystal atoms undergo a transition from cooling to heating when the ion energy is reduced, and for transmission through Si the transition velocities were shown to scale closely with the square root of the ion atomic number. The transition from cooling to heating also depends on the crystallographic direction. Thus for the very open $\langle 110 \rangle$ direction in Si only cooling is observed down to the lowest energies used in the experiments. The strength of the cooling effect was measured as a function of energy for channeling along a $\langle 100 \rangle$ direction in a thin Si crystal. For the lighter ions there is a maximum within the energy interval of our measurements. Measurements with Pt crystals revealed a new behavior: only cooling of well channeled ions, embedded in a depletion zone, was observed for all ions and all energies.

The standard channeling theory cannot explain these effects which violate the rule of reversibility. A mechanism which can account for the observation of cooling of light ions at high velocity is the time-varying screening in ion deflections, stemming from capture and loss of electrons. This explanation is supported by the finding that there is no flux redistribution at very high velocities where all electrons are stripped off the ions. Also, the energies corresponding to maximum strength of the cooling effect scale approximately with the ion atomic number in accordance with expectations based on the charge-exchange model. However, other observations do not have an explanation. Thus the complex behavior of ions with many electrons, especially at lower velocities, is not understood, and also the observed dependence of the phenomena on the atomic number of the crystal presents a challenge.

We have initiated a theoretical approach based on *n*-body classical Monte-Carlo type nN-CTMC simulations for collisions of ions with two parallel strings of atoms. These simulations follow in detail the charge state, and internal excitation of the ion and the deflections in collisions with atoms are calculated explicitly. The preliminary results are in good agreement with measured charge state distributions, and hence it looks promising to continue these time consuming simulations in order learn more about the underlying mechanisms of the flux redistributions and to study more generally the complex behavior of energetic heavy ions in solids.

ACKNOWLEDGMENTS

One of us (F.G.) was supported by the Deutsche Forschungs Gemeinschaft (DFG, under Grant No. AS 102/3-1,2,3). For helpful discussions we are grateful to P. Sigmund. We also want to thank B. Schmidt and J. Chevalier for the production of the crystals without which we could not perform our experiments. This work has been supported by the European Community—Access to Research Infrastructures action of the Improving Human Potential Program - Contract No. HPRI-CT-1999-00019.

[1] D.S. Gemmell, Rev. Mod. Phys. **46**, 129 (1974).

[2] J. Lindhard and V. Nielsen, Mat. Fys. Medd. K. Dan. Vidensk. Selsk. **38**, 9 (1971).

[3] E. Bonderup, H. Esbensen, J.U. Andersen, and H.E. Schiøtt, Radiat. Eff. **12**, 261 (1972).

[4] W. Assmann, H. Huber, S.A. Karamian, F. Grüner, H.D. Mieskes, J.U. Andersen, M. Posselt, and B. Schmidt, Phys. Rev. Lett. **83**, 1759 (1999).

[5] G. Dearnaly, I.V. Mitchell, R.S. Nelson, B.W. Farmery, and M.W. Thompson, Philos. Mag. **18**, 985 (1968).

[6] A.A. Abdurazakov, G.I. Zavyalov, Y.D. Serebro, and V.V. Skvortsov, in *Proceedings of the Seventh International Conference on Atomic Collisions in Solids, Moscow, 1977*, edited by A.F. Tulinov (Moscow State University, Moscow, 1981), pp. 122–124.

[7] F. Grüner, M. Schubert, W. Assmann, F. Bell, S. Karamian, and

J.U. Andersen, Nucl. Instrum. Methods Phys. Res. B **193**, 165 (2002).
[8] J.U. Andersen, F. Grüner, V.A. Ryabov, and A. Uguzzoni, Nucl. Instrum. Methods Phys. Res. B **193**, 188 (2002).
[9] R.E. Olson, J. Ullrich, and H. Schmidt-Böcking, Phys. Rev. A **39**, 5572 (1989).
[10] B. Schmidt, J. von Borany, U. Todt, and A. Erlebach, Sens. Actuators A **41-42**, 689 (1994).
[11] W. Assmann, P. Hartung, H. Huber, P. Staat, H. Steffens, and C. Steinhausen, Nucl. Instrum. Methods Phys. Res. B **85**, 726 (1994).
[12] R.L. Fleischer, P.B. Price, and R.M. Walker, *Nuclear Tracks in Solids* (University of California Press, California, 1975).
[13] G. Rusch, E. Winkel, A. Noll, W. Heinrich, Nucl. Tracks Radiat. Meas. **19**, 261 (1991).
[14] M. Schubert, F. Grüner, W. Assmann, F. Bell, A. Bergmaier, L. Goergens, G. Dollinger, and S. Karamian, Nucl. Instrum. Methods Phys. Res. B **209**, 224 (2003).
[15] G. Dollinger, T. Faestermann, and P. Maier-Komor, Nucl. Instrum. Methods Phys. Res. B **64**, 422 (1992).
[16] H.O. Lutz, S. Datz, C.D. Moak, and T.S. Noggle, Phys. Lett. **33A**, 309 (1970).
[17] K. Shima, N. Kuno, M. Yamanouchi, and H. Tawara, At. Data Nucl. Data Tables **51**, 174 (1992).
[18] S.A. Karamian, W. Assmann, K. Ertl, D. Frischke, H.D. Mieskes, B. Schmidt, and S.P. Tretyakova, Nucl. Instrum. Methods Phys. Res. B **164**, 61 (2000).
[19] S.A. Karamian, F. Grüner, W. Assmann, W. Günther, V.A. Ponomarenko, B. Schmidt, and S.P. Tretyakova, Nucl. Instrum. Methods Phys. Res. B **193**, 144 (2002).
[20] A.B. Wittkower, and H.D. Betz, At. Data Nucl. Data Tables **5**, 120 (1973).
[21] S. Datz, F.W. Martin, C.D. Moak, B.R. Appleton, and L.B. Bridwells, Radiat. Eff. **12**, 163 (1972).
[22] B.R. Appleton, R.H. Ritchie, J.A. Biggerstaff, T.S. Noggle, S. Datz, C.D. Moak, H. Verbeek, and V.N. Neelavathi, Phys. Rev. B **19**, 4347 (1979).
[23] E. Horsdal-Pedersen, P. Loftager, and J. Lahn Rasmussen, J. Phys. B **15**, 4423 (1982).
[24] N. Bohr and J. Lindhard, Mat. Fys. Medd. K. Dan. Vidensk. Selsk. **28**, 7 (1954).
[25] R.E. Olson, J. Ullrich, and H. Schmidt-Böcking, J. Phys. B **20**, L809 (1987).
[26] R. Abrines, and I.C. Percival, Proc. Phys. Soc. London **88**, 861 (1966).
[27] F. Grüner *et al.* (unpublished).